Journal of Building Engineering 34 (2021) 101922

Contents lists available at ScienceDirect

Journal of Building Engineering

journal homepage: http://www.elsevier.com/locate/jobe

# Probabilistic identification of surface recession patterns in heritage buildings based on digital photogrammetry

María L. Jalón [a,*], Juan Chiachío [a,b], Luisa María Gil-Martín [a], Enrique Hernández-Montes [a]

[a] Department of Structural Mechanics and Hydraulic Engineering, University of Granada, Spain
[b] Andalusian Research Institute in Data Science and Computational Intelligence (DaSCI), Granada, Spain

ARTICLE INFO

*Keywords:*
Bayesian system identification
Cultural heritage buildings
Surface recession assessment
Photogrammetric point cloud

ABSTRACT

The deterioration of the built heritage is becoming a pressing issue in many countries. The assessment of such a degradation at large (building) scale is key for maintenance priorisation and decision making. This paper proposes a straightforward yet rigorous method to asses and predict the surface recession in heritage buildings. The method is based on a probabilistic Bayesian approach to identify the most plausible surface recession pattern using digital photogrammetry data. In particular, a set of candidate recession patterns are defined and ranked based on probabilities that measure the relative extent of support of the hypothesised models to the observed data. A real case study for a sixteenth century heritage building in Granada (Spain) is presented. The results show the efficiency of the proposed methodology in identifying not only the most suitable recession pattern for different parts of the building, but also the probability density functions of the basic geometry parameters representing the identified patterns, such as the depth and the height of the surface recession.

## 1. Introduction

The deterioration of Cultural Heritage (CH) sites is one of the biggest challenges in modern societies. Our cultural heritage is degrading faster today than any time in the past [1]. This poses threats not only at a cultural level but also in terms of safety and cost. Countries such as Spain or Italy, along with several others, accrue a significant part of the heritage buildings and structures all over the world, typically made of stone. These countries are increasingly challenged to properly preserve and maintain their important legacy while keeping the associated maintenance costs within reasonable margins.

As a consequence of a number of environmental [2–4] and anthropogenic [5,6] factors, the deterioration of historic masonry structures can be manifested in different ways, one of the most critical being the *surface recession* [7]. This mode of degradation implies a loss of material, which, when acting on safety-critical elements such as buttresses or load-bearing walls, this can severely impair the structural integrity of the entire building. A number of researchers have focused on measuring and modelling the surface recession from different perspectives and disciplines. For example, several mathematical degradation models have been proposed to predict the degree of deterioration of the heritage building materials. A good literature review is provided by Sabas et al. [8] focusing on calcareous stone degradation. Other researchers have focused on experimental approaches using advanced structural health monitoring (SHM) techniques [9–11], photogrammetry [12,13], laser scanning [14] or radiometric methods [15–17] to measure the degree of deterioration of CH elements so as to support decision making about preventive maintenance [18], restoration [19–22], and resilience to climate change [23].

As evident from the literature, most of the contributions focus on physicochemical material deterioration rather than on higher-scale structural-level degradation, which is closely related with the actual structural integrity of the building. Furthermore, any individual heritage building can be viewed as a collection of complex and integrated subsystems with possibly different building materials, each one with its own history of deterioration and its own history of treatments and restoration. Such spatial and temporal variability implies irreducible uncertainty that needs to be considered for a rigorous degradation assessment. This uncertainty not only includes uncertain model parameters for a particular surface recession pattern, but also *epistemic uncertainty* [24] coming from the adoption of a particular pattern among a set of candidates. In this sense, probabilistic instead of deterministic approaches need to be adopted for an effective yet rigorous surface recession assessment. Probabilistic approaches have been successfully applied for

* Corresponding author.
*E-mail address:* mljalon@ugr.es (M.L. Jalón).

https://doi.org/10.1016/j.jobe.2020.101922
Received 20 June 2020; Received in revised form 12 September 2020; Accepted 23 October 2020
Available online 6 November 2020

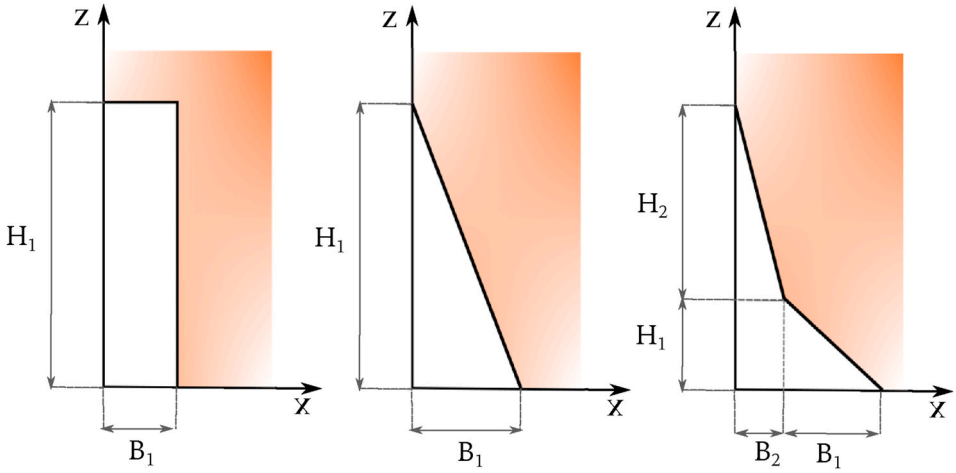


**Fig. 1.** Candidate surface recession patterns: $\mathcal{M}_1$ = rectangular (left), $\mathcal{M}_2$ = triangular (centre), and $\mathcal{M}_3$ = bilineal (right).

**Fig. 2.** Photogrammetric point cloud representation of the buttress. San Jerónimo Monastery.

uncertainty quantification in the context of degradation assessment and parameter identification in metals [25–28], thermal conductivity assessment [29], and fatigue in composite materials [30,31], among others. However, to the authors' best knowledge, the identification of higher-scale geometry degradation patterns in cultural heritage buildings including assessment of their main governing parameters using a full probabilistic approach has not been covered in the literature before.

In this paper, a rational probabilistic methodology for surface recession assessment based on a simple non-destructive technique such as digital photogrammetry is proposed. The proposed method is based on solid Bayesian system identification principles [32,33] allowing the identification of the most plausible surface recession pattern among a set of candidates for a given photogrammetric dataset. The plausibility of the various possibilities is expressed through probabilities that measure the relative *degree of belief* of the candidate geometry degradation patterns conditional to the available data. The candidate patterns are defined as simple geometric forms such as those depicted in Fig. 1, so that these can be subsequently used as geometry inputs in subsequent structural integrity analyses. In this sense, the surface recession patterns become geometrically defined by basic parameters such as the height and the depth of the degradation. Should more complex geometry degradation patterns were identified (e.g., a staircase function), these might require additional parameters for their complete univocal geometrical characterisation.

Apart from recession pattern identification, the proposed methodology provides as output the probability density functions (PDFs) of the basic geometric degradation parameters (e.g., height and depth) of the assessed patterns. These PDFs denote the *epistemic uncertainty* (i.e., uncertainty reducible in the light of new information) due not only to the lack of enough data, but also to the idealisation of the physical reality using a simple geometrical model. The PDFs of the degradation parameters are subsequently used to provide a probabilistic estimation of the rate of degradation of the analysed element (e.g., a load bearing façade), having the element's age as known. The methodology has been

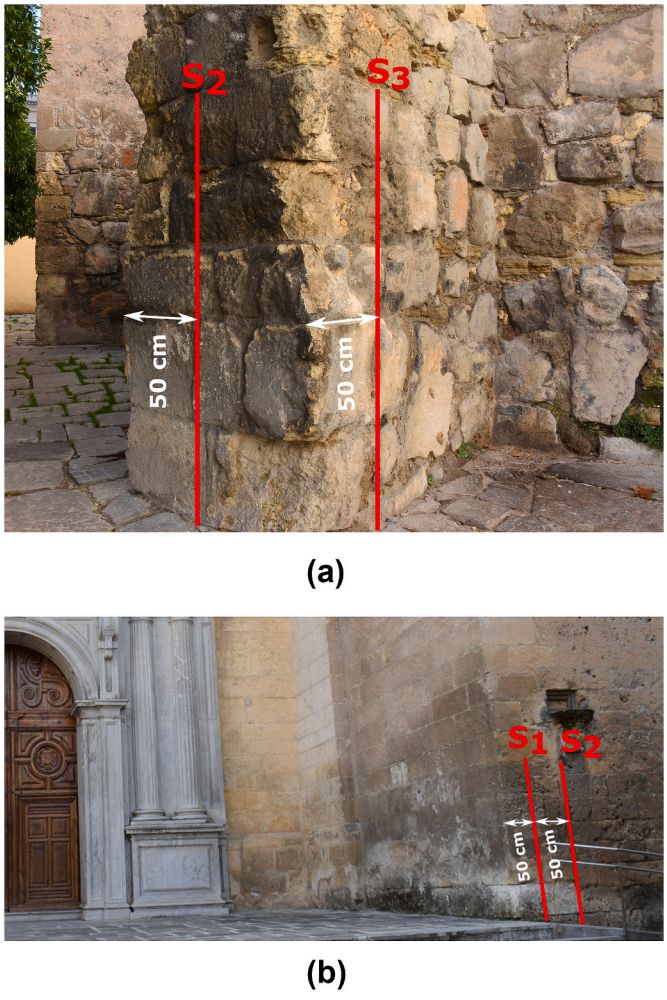


**Fig. 3.** Location of the degradation profiles in the building: (a) buttress (section $S_1$ located on the hidden side in the picture), (b) main façade.

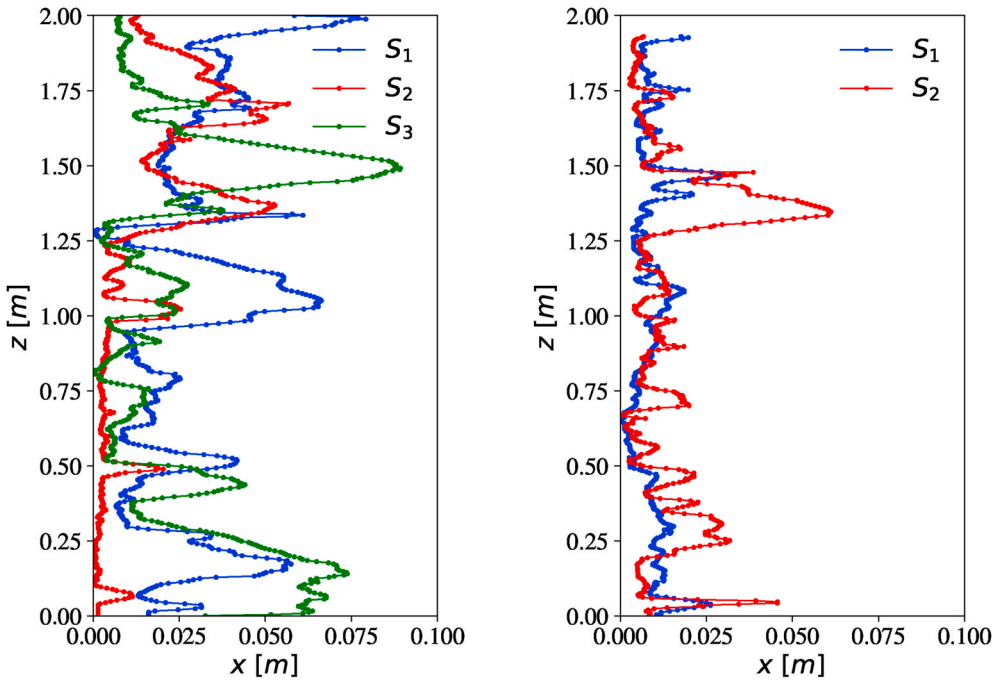


**Fig. 4.** Measured degradation profiles of (a) the buttress, and (b) the main façade of San Jerónimo Monastery.

**Table 1**
Prior information of model parameters for each surface degradation hypothesis.

| Model class | Degradation pattern | $\theta_1$ | $\theta_2$ | $\theta_3$ | $\theta_4$ | $\theta_5$ |
|---|---|---|---|---|---|---|
| $\mathcal{M}_1$ | Square | $B_1$ | $H_1$ | $\sigma_e$ | −− | −− |
| Prior PDF | $p(\boldsymbol{\theta}\|\mathcal{M}_1)$ | $\mathcal{U}(0, 0.2)$ | $\mathcal{U}(0, 2)$ | $\mathcal{U}(5e-3, 5e-1)$ | −− | −− |
| $\mathcal{M}_2$ | Triangle | $B_1$ | $H_1$ | $\sigma_e$ | −− | −− |
| Prior PDF | $p(\boldsymbol{\theta}\|\mathcal{M}_2)$ | $\mathcal{U}(0, 0.2)$ | $\mathcal{U}(0, 2)$ | $\mathcal{U}(5e-3, 5e-1)$ | −− | −− |
| $\mathcal{M}_3$ | Bilineal | $B_1$ | $B_2$ | $H_1$ | $H_2$ | $\sigma_e$ |
| Prior PDF | $p(\boldsymbol{\theta}\|\mathcal{M}_3)$ | $\mathcal{U}(0, 0.1)$ | $\mathcal{U}(0, 0.1)$ | $\mathcal{U}(0,1)$ | $\mathcal{U}(0, 1)$ | $\mathcal{U}(5e-3, 5e-1)$ |

illustrated using digital photogrammetry data for the San Jerónimo Monastery, a sixteenth century CH building in Granada (Spain), considering two different elements, namely (1) a buttress, and (2) the main façade. For this case study, three candidate geometry degradation patterns are considered for illustration purposes, as depicted in Fig. 1. The results confirm the suitability and efficiency of the method in identifying plausible surface recession patterns and providing useful geometry degradation-related information using just a simple non-sophisticated digital photography equipment.

The remainder of the paper is organised as follows: Section 2 describes the proposed Bayesian methodology to identify the most plausible geometric degradation pattern out of digital photogrammetry data. In Section 3, the proposed methodology is illustrated and tested for San Jerónimo Monastery's 3D photogrammetry model. Section 4 provides the conclusions and future works that can be derived from this research.

## 2. Methodology

### 2.1. Bayesian degradation pattern recognition

A Bayesian model class selection framework [32,34] is developed in this section for a rigorous and robust identification of the most plausible surface recession pattern. A set of $N_m = 3$ candidate degradation profiles or *model classes* $\mathbf{M} = \{\mathcal{M}_j\}_{j=1}^{N_m}$ are initially proposed, as shown in Fig. 1.

These model classes are regarded as hypothesised surface recession patterns which are considered as equally plausible a priori, i.e., $P(\mathcal{M}_j|\mathbf{M}) = 1/N_m$. After assimilating these model classes with the experimental data, the hypothesised degradation profiles are ranked based on *posterior probabilities* $P(\mathcal{M}_j|\mathcal{D}, \mathbf{M})$ which express the relative degree of belief of the hypothesised geometric degradation patterns in representing the data $\mathcal{D}$ [32]. To this end, a probabilistic description of a candidate degradation pattern is obtained by introducing an uncertain error term $\mathbf{e}$ that measures the discrepancy between the hypothesised degradation profile given by $\boldsymbol{\theta}$, denoted by $\mathbf{z}_{\mathcal{M}}(\boldsymbol{\theta})$, and the measured degradation profile $\mathbf{z}_{\mathcal{D}}$, as follows:

$$\mathbf{z}_{\mathcal{D}} = \mathbf{z}_{\mathcal{M}}(\boldsymbol{\theta}) + \mathbf{e} \tag{1}$$

Following the Principle of Maximum Information Entropy [35], a zero mean Gaussian distribution is conservatively adopted to model the error term $\mathbf{e}$ such that it produces the largest uncertainty [32]. Thus, the measured data $\mathbf{z}_{\mathcal{D}}$ will be represented by $\mathbf{z}_{\mathcal{M}}(\boldsymbol{\theta})$ under model class $\mathcal{M}_j$ with a probability density

$$p(\mathbf{z}_{\mathcal{D}}|\boldsymbol{\theta}, \mathcal{M}_j) = \left(2\pi\sigma_e^2\right)^{-\frac{N_s}{2}} \exp\left(-\frac{1}{2}\left(\frac{\mathcal{J}(\boldsymbol{\theta})}{\sigma_e}\right)^2\right) \tag{2}$$

where $\mathcal{J}(\boldsymbol{\theta})$ is a goodness-of-fit function which is defined as the $\ell_2$-norm of the measured and modelled data, as: $\mathcal{J}(\boldsymbol{\theta}) = \left(\sum_{i=1}^{N_s}(z_{i,\mathcal{M}}^{-1} - z_{i,\mathcal{D}}^{-1})^2\right)^{1/2}$,

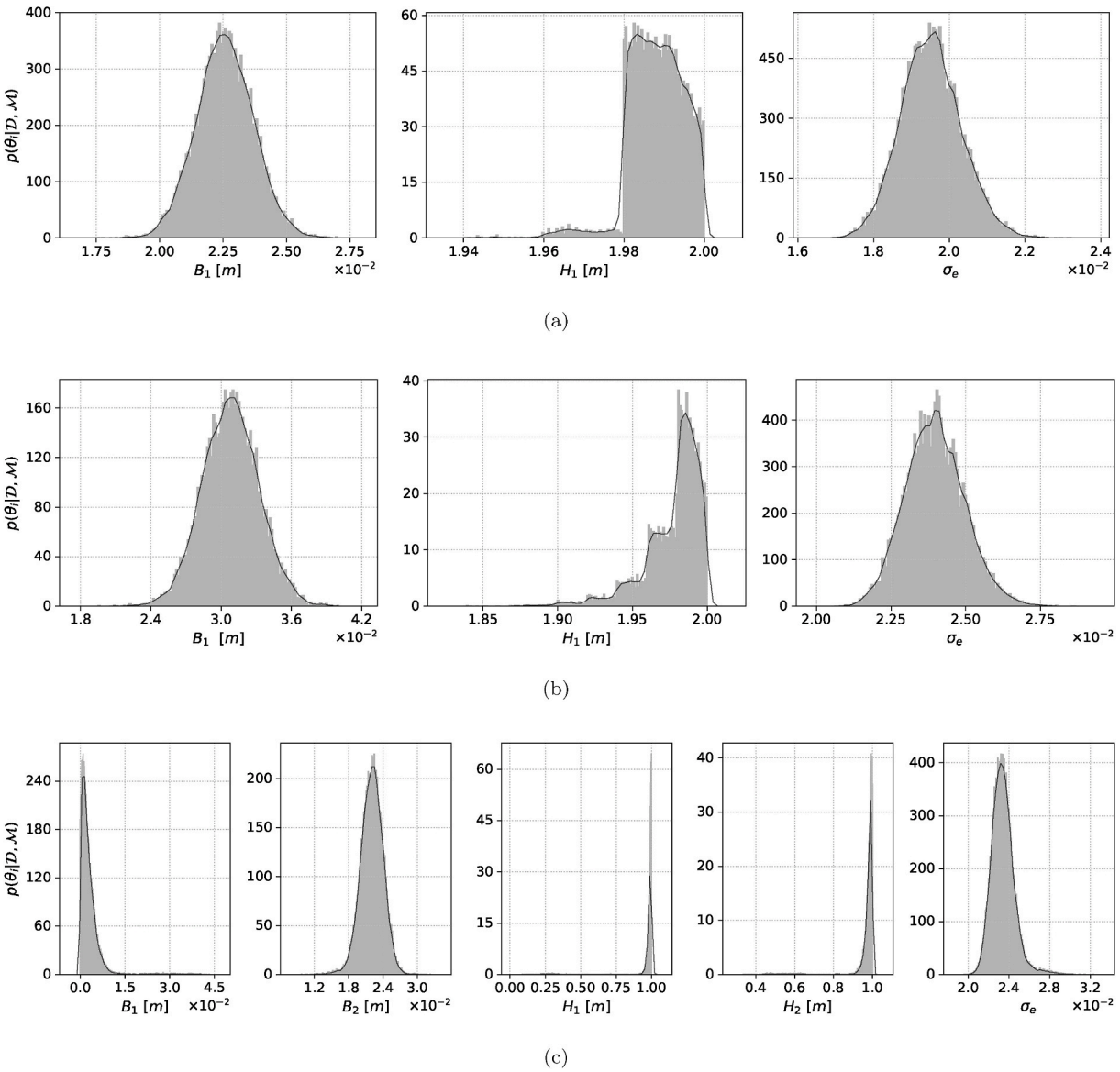


**Fig. 5.** Posterior probability density functions of the model parameters defining the candidate surface recession patterns: a) $\mathcal{M}_1$ = Square, (b) $\mathcal{M}_2$ = Triangular, (c) $\mathcal{M}_3$ = Bilineal. Results correspond to the buttress of San Jerónimo Monastery.

**Table 2**
Mean and coefficient of variation of the posterior model parameters defining surface patterns $\mathcal{M}_1$ to $\mathcal{M}_3$, estimated from samples of the marginal posterior PDFs. Results correspond to the main façade of San Jerónimo Monastery.

| | | Degradation parameters | | | | Error parameter |
|---|---|---|---|---|---|---|
| | | $B_1$ | $B_2$ | $H_1$ | $H_2$ | $\sigma_v$ |
| $\mathcal{M}_1$ | mean | 0.0113 | –– | 1.9629 | –– | 0.0098 |
| | C.O.V | 0.0628 | –– | 0.0293 | –– | 0.0517 |
| $\mathcal{M}_2$ | mean | 0.0170 | –– | 1.9706 | –– | 0.0112 |
| | C.O.V | 0.0810 | –– | 0.0132 | –– | 0.0513 |
| $\mathcal{M}_3$ | mean | 0.0017 | 0.0121 | 0.9524 | 0.9546 | 0.0110 |
| | C.O.V | 1.2327 | 0.0934 | 0.1412 | 0.091 | 0.0682 |

with $z_{i,\mathcal{M}}^{-1}$ and $z_{i,\mathcal{D}}^{-1}$ being the abscissa image of the $i$-th element of the vectors $\mathbf{z}_{\mathcal{M}}$ and $\mathbf{z}_{\mathcal{D}}$, respectively, and $\sigma_e$ is the standard deviation of the $i$-th component of the model error $\mathbf{e}$, with $i = 1, \ldots N_s$.

To formally define the model class $\mathcal{M}_j$, the prior distribution of the model parameters $p(\boldsymbol{\theta}|\mathcal{M}_j)$ also needs to be provided. These are basic geometric degradation parameters such as the height and the depth of degradation; i.e., $\boldsymbol{\theta} = \{B_1, H_1\}$ for model classes $\mathcal{M}_1$ and $\mathcal{M}_2$, and $\boldsymbol{\theta} = \{B_1, B_2, H_1, H_2\}$ for $\mathcal{M}_3$. Next, the posterior distribution of these model parameters $p(\boldsymbol{\theta}|\mathcal{D}, \mathcal{M}_j)$ given the data $\mathcal{D} \triangleq \mathbf{z}_{\mathcal{D}}$ for a specific model class $\mathcal{M}_j$, can be obtained using Bayes' Theorem, as follows:

$$p(\boldsymbol{\theta}|\mathcal{D}, \mathcal{M}_j) = \frac{p(\mathcal{D}|\boldsymbol{\theta}, \mathcal{M}_j)p(\boldsymbol{\theta}|\mathcal{M}_j)}{p(\mathcal{D}|\mathcal{M}_j)} \tag{3}$$

where $p(\mathcal{D}|\boldsymbol{\theta}, \mathcal{M}_j)$ denotes the *likelihood function* represented by Equation (2) and $p(\mathcal{D}|\mathcal{M}_j)$ is the *evidence* of model class $\mathcal{M}_j$ in representing the data $\mathcal{D}$. The computation of Equation (3) is analytically intractable in most of the cases, requiring stochastic simulation methods to numerically address it. In this case, the Metropolis-Hastings (M-H) algorithm [36,37] is adopted for its simplicity and efficiency to solve Equation (3) by obtaining samples from the posterior distribution $p(\boldsymbol{\theta}|\mathcal{D}, \mathcal{M}_j)$.

Finally, the model classes (i.e., hypothesised degradation profiles) are ranked according to their posterior plausibilities $P(\mathcal{M}_j|\mathcal{D}, \mathbf{M})$, obtained through Bayes' Theorem as follows:

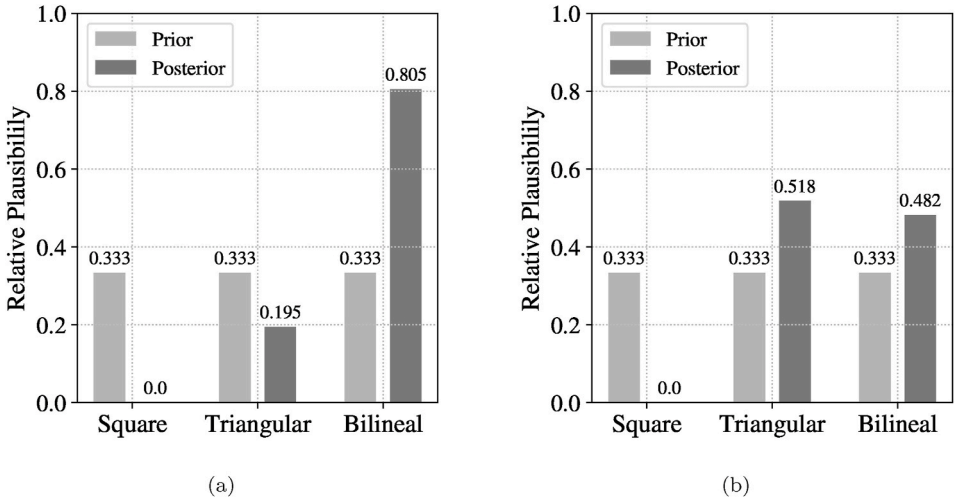


**Fig. 6.** Surface recession pattern ranking based on posterior probabilities for (a) the buttress, and (b) the main façade of San Jerónimo Monastery.

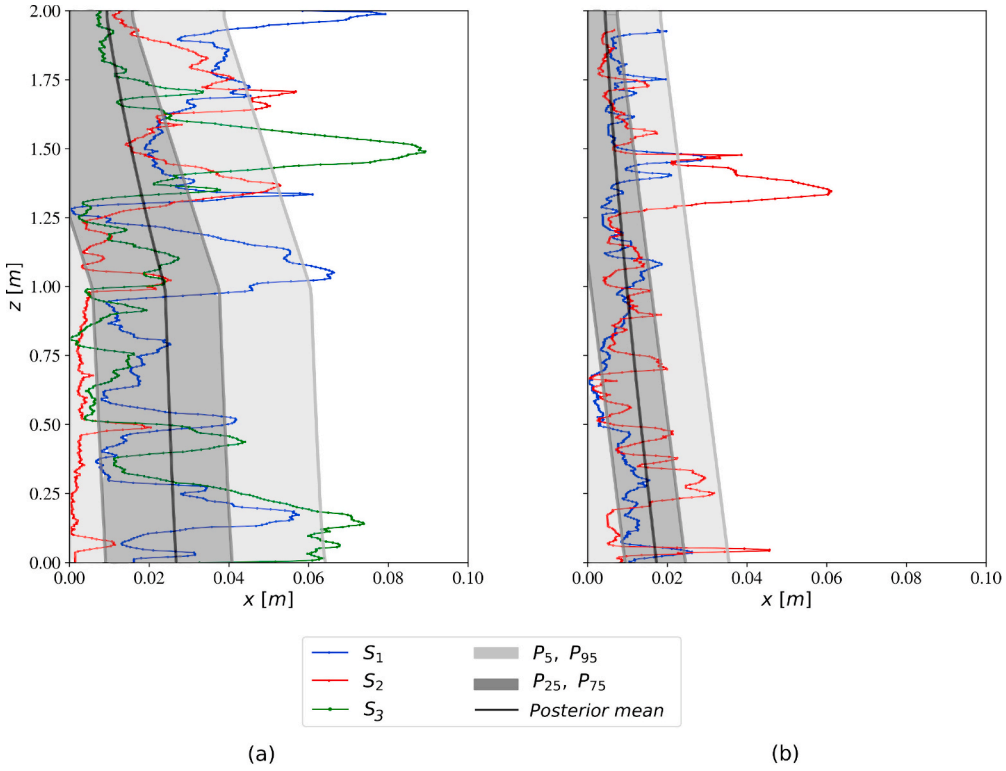


**Fig. 7.** Posterior mean degradation and confidence intervals ($P_5$, $P_{25}$, $P_{75}$, $P_{95}$) under the most plausible degradation pattern against the experimental degradation data ($S_1$, $S_2$, $S_3$) for (a) the buttress, and (b) the main façade of San Jerónimo Monastery.

$$P(\mathcal{M}_j|\mathcal{D},\mathbf{M}) = \frac{p(\mathcal{D}|\mathcal{M}_j)P(\mathcal{M}_j|\mathbf{M})}{\Sigma_{l=1}^{N_m} p(\mathcal{D}|\mathcal{M}_l)P(\mathcal{M}_l|\mathbf{M})} \tag{4}$$

where $P(\mathcal{M}_j|\mathbf{M}) = 1/N_m$ is the prior probability of the model class $\mathcal{M}_j$, and $p(\mathcal{D}|\mathcal{M}_j)$ is the evidence of the model class. This evidence can be obtained by using the Total Probability Theorem:

$$p(\mathcal{D}|\mathcal{M}_j) = \int_\Theta \underbrace{p(\mathcal{D}|\boldsymbol{\theta},\mathcal{M}_j)}_{\text{Eq. (2)}} p(\boldsymbol{\theta}|\mathcal{M}_j)d\boldsymbol{\theta} \tag{5}$$

where $p(\boldsymbol{\theta}|\mathcal{M}_j)$ is the prior PDF of model parameters $\boldsymbol{\theta}$. Note that the evaluation of the multi-dimensional integral in Equation (5) is nontrivial in most of the cases. One straightforward way to approximate the evidence that is adopted in this paper is by considering the probability integral in Equation (5) as a mathematical expectation of the likelihood $p(\mathcal{D}|\boldsymbol{\theta},\mathcal{M}_j)$ with respect to the prior $p(\boldsymbol{\theta}|\mathcal{M}_j)$. This approach leads to the direct Monte Carlo method as follows:

$$p(\mathcal{D}|\mathcal{M}_j) \approx \frac{1}{K}\sum_{k=1}^{K} p(\mathcal{D}|\boldsymbol{\theta}^{(k)},\mathcal{M}_j) \tag{6}$$

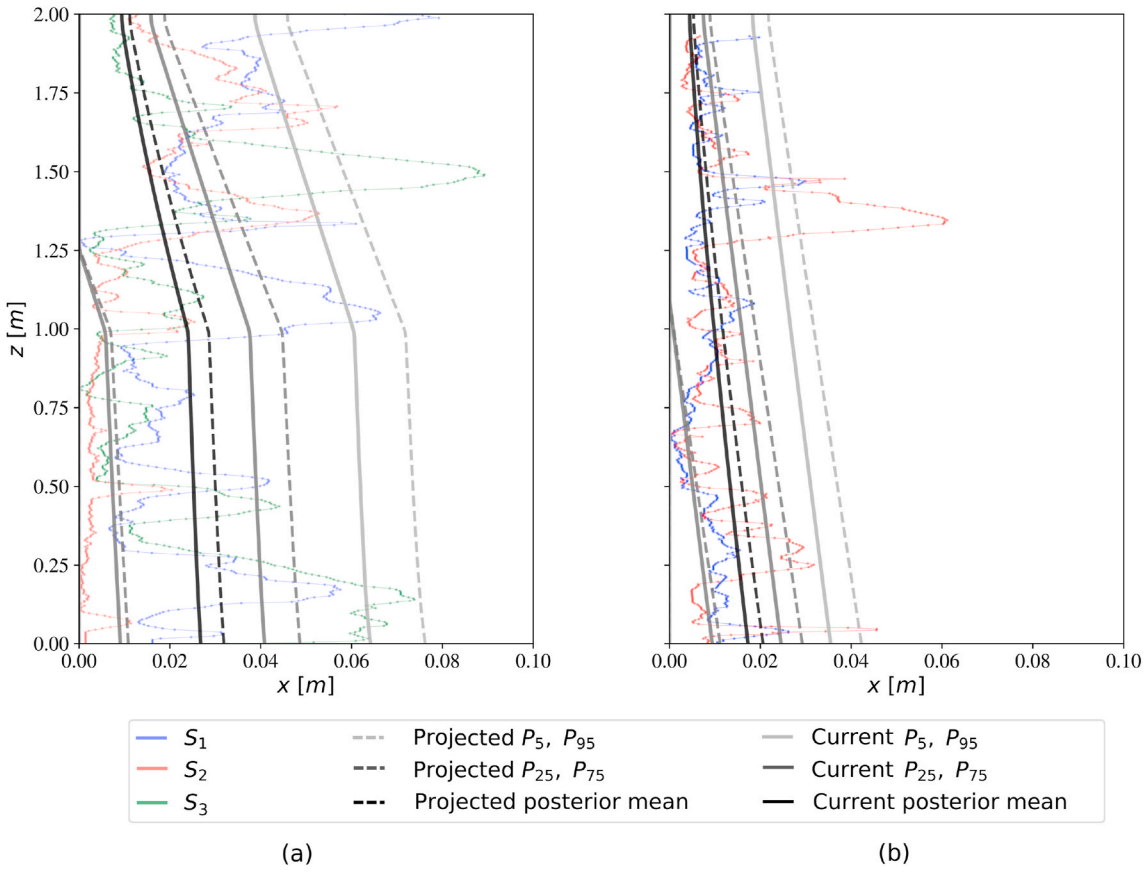


**Fig. 8.** Current and prognosticated posterior mean degradation and confidence intervals ($P_5$, $P_{25}$, $P_{75}$, $P_{95}$) against the experimental degradation data ($S_1$, $S_2$, $S_3$) for (a) the buttress, and (b) the main façade of San Jerónimo Monastery.

where the $\boldsymbol{\theta}^{(k)}$ are $K$ samples drawn from the prior $p(\boldsymbol{\theta}|\mathcal{M}_j)$.

**Algorithm 1.** Bayesian model class selection

**Algorithm 1:** Bayesian model class selection

1 Define ▷ $\mathbf{M} = \{\mathcal{M}_j\}_{j=1}^{N_m}$ and $P(\mathcal{M}_j|\mathbf{M})$ ; // Model classes
2 Define ▷ $\boldsymbol{\theta}$ and $p(\boldsymbol{\theta}|\mathcal{M}_j)$ $\forall \mathcal{M}_j \in \mathbf{M}$ ; // Model parameters and prior PDFs
3 **for** $j = 1$ **to** $N_m$ **do**
4 Obtain $p(\boldsymbol{\theta}|\mathcal{D}, \mathcal{M}_j) \sim$ M-H algorithm in Appendix A ; // Posterior PDFs
5 Estimate $p(\mathcal{D}|\mathcal{M}_j) \sim$ Eq. (6) ; // Evidence
6 **end**
7 Obtain $p(\mathcal{M}_j|\mathcal{D}, \mathbf{M}) \sim$ Eq. (4);
8 Select the most plausible $\mathcal{M}^* = \arg\max p(\mathcal{M}_j|\mathcal{D}, \mathbf{M})$ ;

### 2.2. Implementation details

The proposed Bayesian framework for surface recession pattern identification is described here at an algorithmic level. For each surface degradation pattern (e.g., model class $\mathcal{M}$), the posterior PDFs of the model parameters are obtained using the M-H algorithm and then the evidence is calculated according to Equation (6). Once the evidences of the candidate geometric degradation patterns are obtained, their relative posterior plausibilities are computed according to Equation (4), and the most probable one is selected. An algorithmic implementation of the proposed Bayesian surface recession patterns identification methodology is provided in Algorithm 1.

To obtain the posterior PDF $p(\boldsymbol{\theta}|\mathcal{D}, \mathcal{M})$ (step 4 in Algorithm 1), the M-H algorithm generates samples from a specially constructed Markov chain whose stationary distribution is the required posterior PDF. By sampling a candidate model parameter $\boldsymbol{\theta}'$ from a proposal distribution $q(\boldsymbol{\theta}'|\boldsymbol{\theta}^{\zeta})$, the M-H obtains the state of the chain at $\zeta + 1$, given the state at $\zeta$, specified by $\boldsymbol{\theta}^{\zeta}$. The candidate parameter $\boldsymbol{\theta}'$ is accepted (i.e., $\boldsymbol{\theta}^{\zeta+1} = \boldsymbol{\theta}'$) with probability $\min\{1, r\}$, and rejected (i.e., $\boldsymbol{\theta}^{\zeta+1} = \boldsymbol{\theta}^{\zeta}$) with the remaining probability $1 - \min\{1, r\}$, where:

$$r = p(\mathcal{D}|\boldsymbol{\theta}', \mathcal{M})p(\boldsymbol{\theta}'|\mathcal{M})q(\boldsymbol{\theta}^{\zeta}|\boldsymbol{\theta}')/p(\mathcal{D}|\boldsymbol{\theta}^{\zeta}, \mathcal{M})p(\boldsymbol{\theta}^{\zeta}|\mathcal{M})q(\boldsymbol{\theta}'|\boldsymbol{\theta}^{\zeta}) \tag{7}$$

The process is repeated until $T_s$ samples have been generated so that the

monitored acceptance rate (ratio between accepted M-H samples over total amount of samples) reaches an asymptotic behaviour. A pseudo-code description of this method is provided as Algorithm 2.

**Algorithm 2.** M-H algorithm

**Algorithm 2:** M-H algorithm

Initialize $\boldsymbol{\theta}^{\zeta=0}$ by sampling from the prior PDF: $\boldsymbol{\theta}^0 \sim p(\boldsymbol{\theta}|\mathcal{M})$;
**for** $\zeta = 1$ **to** $T_s$ **do**
  Sample from the proposal: $\boldsymbol{\theta}' \sim q(\boldsymbol{\theta}'|\boldsymbol{\theta}^{\zeta-1})$;
  Compute $r$ from Eq. (A.1);
  Generate a uniform random number: $\alpha \sim \mathcal{U}[0,1]$;
  **if** $r \geqslant \alpha$ **then**
    Set $\boldsymbol{\theta}^{\zeta} = \boldsymbol{\theta}'$;
  **else**
    Set $\boldsymbol{\theta}^{\zeta} = \boldsymbol{\theta}^{\zeta-1}$;
  **end**
**end**

## 3. Case studies

The Bayesian methodology for degradation pattern assessment proposed in this paper is illustrated here for a cultural heritage building in Granada (Spain), the San Jerónimo Monastery. In particular, two different structural elements of the building, namely the main façade and the buttresses, are investigated.

Degradation profiles of these elements are taken from digital photogrammetry data using a digital still camera (Nikon D7200, 18 mm focal length). The images are post-processed using Agisoft Metashape [38], a software that performs photogrammetric processing out of digital images and generates 3D spatial data known as *photogrammetric point cloud* (PPC), which is shown in Fig. 2.

For the buttress, one section at each of the three faces of the element are selected (Fig. 3a). As for the main façade, two sections separated by 50 cm each are considered (Fig. 3b). The photogrammetric data is obtained up to 2 m above the ground level since the upper part of the building does not show a relevant deterioration. Therefore a zero deterioration depth is hypothesised above 2 m hight, which is adopted as the reference for the measurements.

The degradation profiles are obtained out of the PPC using the open source software CloudCompare [39], and are represented as relative distances in Fig. 4.

In both cases, the heterogeneity and complexity of the measured degradation profiles in Fig. 4 become evident, which prevent us from selecting a particular degradation pattern just by observing the data. Instead, the most suitable surface recession pattern for the measured data is identified using the proposed Bayesian methodology.

As explained in Section 2, three model classes ($N_m = 3$) are considered for the assessment, as depicted in Fig. 1. The prior information of the model parameters representing the model classes is summarised in Table 1. Note that the standard deviation of the prediction error $\sigma_e$ is assumed to be part of the set of uncertain parameters $\boldsymbol{\theta}$ of each model class, with an uniform prior distribution $\sigma_e = \mathcal{U}(5\text{e}-3, 5\text{e}-1)$ for every model class.

Based on Bayes' Theorem in Equation (3), samples from the posterior PDFs of the model parameters are obtained based on the M-H algorithm (Algorithm 2) using $T_s = 100{,}000$ samples and a Gaussian proposal distribution $q(\boldsymbol{\theta}^{*}|\boldsymbol{\theta}^{\zeta}) = \mathcal{N}(\boldsymbol{\theta}^{\zeta}, \boldsymbol{\Sigma})$, where $\boldsymbol{\Sigma}$ is the covariance matrix of the random walk. Given that the model parameters are assumed to be stochastically independent a priori, $\boldsymbol{\Sigma}$ is a diagonal matrix, i.e., $\boldsymbol{\Sigma} = diag(\sigma^2_{\theta_1}, \ldots, \sigma^2_{\theta_n})$, and each individual parameter in $\boldsymbol{\theta}$ performs an independent random walk. The diagonal elements of $\boldsymbol{\Sigma}$ are appropriately selected through initial test runs such that the monitored acceptance rate is within the suggested range $\bar{r} \in [0.2, 0.4]$ for M-H algorithm [40, 41]. The resulting marginal posterior PDFs of the model parameters for each model class are represented in Fig. 5 for the data corresponding to the buttress of San Jerónimo Monastery (Fig. 4a). For the façade data (Fig. 4b), the posterior results are summarised in Table 2. Observe that the proposed methodology provides full probabilistic description of the basic geometric degradation parameters describing each model class.

Next, the relative plausibilities of the candidate degradation patterns are computed following Equation (4). The results are shown in Fig. 6 for the two datasets. Note that model class $\mathcal{M}_3$ (Bilineal) is revealed as the most plausible to represent the degradation of the buttress, since it provides the highest posterior probability ($P(\mathcal{M}_3|\mathbf{M}) = 0.805$). As for the façade data, both the triangular and bilinear degradation models render very similar posterior probabilities, namely $P(\mathcal{M}_2|\mathbf{M}) = 0.518$ and $P(\mathcal{M}_3|\mathbf{M}) = 0.482$, so the choice of any of them would be appropriate. However, for this particular case, the adoption of the most simpler one (triangular pattern) would lead to a parsimonious model selection.

For illustrative purposes, forward model simulation results are provided using the posterior PDFs of the model parameters as inputs for the stochastic degradation model in Equation (2). Results are shown in Fig. 7 for the two case studies and the most plausible model class. It can be observed that the variability and complexity in the data are translated as uncertainty in the input parameters so that when simulated, the model output properly represents the variability observed in the data.

Finally, apart from a simulation of the current degradation state, an estimate of the degradation over the next hundred years has been prognosticated. This prediction has been carried out by assuming a constant recession rate over the five centuries of the building. Results are shown in Fig. 8. This information can be subsequently used in a suitable structural model to obtain a prediction ahead in time of the structural integrity of the building assuming a constant degradation rate over the time.

## 4. Conclusions

A Bayesian methodology for surface recession pattern assessment and ranking in heritage buildings based on digital photogrammetry data was presented in this paper. The methodology allows accounting for several sources of uncertainty; in particular, the epistemic uncertainty due to choice of a particular geometric degradation pattern among a set of candidates, and the uncertainty coming from the complexity and variability of the measured data. Apart from the identification of the current surface recession state with quantified uncertainty, the methodology enables an estimation of the future surface recession over the time assuming a constant degradation rate. The suitability and effectiveness of the method was shown through a real case study using

photogrammetry data from the sixteenth century San Jerónimo Monastery in Granada (Spain). The results confirm the efficiency of the method in providing useful geometric degradation information using a non-sophisticated digital photography equipment, which can be easily used as input for subsequent structural integrity analyses. As a drawback, the proposed methodology considers geometry degradation only disregarding other deterioration processes such as chemical changes, biodeterioration, or other lower-scale damages such as surface cracks. However, the combination or even the fusion of the proposed methodology with higher resolution techniques such as multi-spectral image analysis within a proper methodological framework could greatly overcome such a limitation. This may constitute a relevant and desirable extension of the proposed research.

## Author statement

María L. Jalón: Formal analysis, Software, Data curation. Juan Chiachío: Methodology, Writing- Original draft preparation. Luisa María Gil-Martín: Supervising, Writing-Review & Editing. Enrique Hernández-Montes: Conceptualisation, Funding acquisition, Project administration.

## Declaration of competing interest

The authors declare that they have no known competing financial interests or personal relationships that could have appeared to influence the work reported in this paper.

## Acknowledgements

This work is part of the HYPERION project (https://www.hyperion-project.eu/). HYPERION has received funding from the European Union's Framework Programme for Research and Innovation (Horizon 2020) under grant agreement no. 821054. The content of this publication is the sole responsibility of UGR and does not necessarily reflect the opinion of the European Union.

## Appendix A. Supplementary data

Supplementary data to this article can be found online at https://doi.org/10.1016/j.jobe.2020.101922.

## References

[1] G. Burns, Deterioration of our cultural heritage, Nature 352 (6337) (1991) 658–660.
[2] S. Fatorić, E. Seekamp, Are cultural heritage and resources threatened by climate change? A systematic literature review, Climatic Change 142 (1–2) (2017) 227–254.
[3] S. Salvini, Deterioration of carbonate rocks and vulnerability of cultural heritage in a changing climate, PhD. Thesis, University of Padova, Italy, 2017. Dipartimento di Geoscienze.
[4] F. Vidal, R. Vicente, J.M. Silva, Review of environmental and air pollution impacts on built heritage: 10 questions on corrosion and soiling effects for urban intervention, J. Cult. Herit. 37 (2019) 273–295.
[5] S. Siegesmund, T. Weiss, A. Vollbrecht, Natural stone, weathering phenomena, conservation strategies and case studies: introduction, Geol. Soc. Lond. Spec. Publ. 205 (1) (2002) 1–7.
[6] N. Prieto-Taboada, I. Ibarrondo, O. Gómez-Laserna, I. Martinez-Arkarazo, M. A. Olazabal, J.M. Madariaga, Buildings as repositories of hazardous pollutants of anthropogenic origin, J. Hazard Mater. 248 (2013) 451–460.
[7] P. Maravelaki, R. Bertoncello, G. Biscontin, G. Battaglin, E. Zendri, E. Tondello, Investigations of the surface processes on exposed limestones, MRS Online Proceedings Library Archive 267 (1992).
[8] M. Saba, E.E. Quiñones-Bolaños, A.L.B. López, A review of the mathematical models used for simulation of calcareous stone deterioration in historical buildings, Atmos. Environ. 180 (2018) 156–166.
[9] A. Moropoulou, K.C. Labropoulos, E.T. Delegou, M. Karoglou, A. Bakolas, Non-destructive techniques as a tool for the protection of built cultural heritage, Construct. Build. Mater. 48 (2013) 1222–1239.
[10] M.G. Masciotta, J.C.A. Roque, L.F. Ramos, P.B. Lourenço, A multidisciplinary approach to assess the health state of heritage structures: the case study of the church of monastery of Jerónimos in Lisbon, Construct. Build. Mater. 116 (2016) 169–187.
[11] N. Işık, F.M. Halifeoğlu, S. Ipek, Nondestructive testing techniques to evaluate the structural damage of historical city walls, Construct. Build. Mater. 253 (2020) 119228.
[12] M.A. Núñez-Andrés, F. Buill, A. Costa-Jover, J.M. Puche, Structural assessment of the roman wall and vaults of the cloister of Tarragona Cathedral, J. Build. Eng. 13 (2017) 77–86.
[13] L. de Ferri, C. Santagati, M. Catinoto, E. Tesser, E.M. di San Lio, G. Pojana, A multi-technique characterization study of building materials from the Exedra of S. Nicolò l'Arena in Catania (Italy), J. Build. Eng. 23 (2019) 377–387.
[14] E. Costamagna, M.S. Quintero, N. Bianchini, N. Mendes, P.B. Lourenço, S. Su, Y. M. Paik, A. Min, Advanced non-destructive techniques for the diagnosis of historic buildings: the Loka-Hteik-Pan temple in Bagan, J. Cult. Herit. 43 (2020) 108–117.
[15] M. Hemmleb, F. Weritz, A. Schiemenz, A. Grote, C. Maierhofer, Multi-spectral Data Acquisition and Processing Techniques for Damage Detection on Building Surfaces, Image Engineering and Vision Metrology, Dresden, Germany, 2006.
[16] J.L. Lerma, M. Cabrelles, C. Portales, Multitemporal thermal analysis to detect moisture on a building façade, Construct. Build. Mater. 25 (5) (2011) 2190–2197.
[17] J. Valença, L.M.S. Gonçalves, E.N.B. S Júlio, Damage assessment on concrete surfaces using multi-spectral image analysis, Construct. Build. Mater. 40 (2013) 971–981.
[18] H.E. Silva, F.M.A. Henriques, Preventive conservation of historic buildings in temperate climates. The importance of a risk-based analysis on the decision-making process, Energy Build. 107 (2015) 26–36.
[19] T.S. Bozkurt, B. Sayin, C. Akcay, B. Yildizlar, N. Karacay, Restoration of the historical masonry structures based on laboratory experiments, J. Build. Eng. 7 (2016) 343–360.
[20] A. Formisano, A. Marzo, Simplified and refined methods for seismic vulnerability assessment and retrofitting of an Italian cultural heritage masonry building, Comput. Struct. 180 (2017) 13–26.
[21] J.R. Rey, P.V. González, J.R. Carmona, Structural refurbishment strategies on industrial heritage buildings in Madrid: recent examples, Hormigón y Acero 69 (285) (2018) e27–e35.
[22] E.M. Alonso-Villar, T. Rivas, J.S. Pozo-Antonio, Adhesives applied to granite cultural heritage: effectiveness, harmful effects and reversibility, Construct. Build. Mater. 223 (2019) 951–964.
[23] A.J. Prieto, K. Verichev, M. Carpio, Heritage, Resilience and Climate Change: A Fuzzy Logic Application in Timber-Framed Masonry Buildings in Valparaíso, Chile, Building and Environment, 2020, p. 106657.
[24] S. Sankararaman, S. Mahadevan, Model validation under epistemic uncertainty, Reliab. Eng. Syst. Saf. 96 (9) (2011) 1232–1241.
[25] R. Zhang, S. Mahadevan, Model uncertainty and Bayesian updating in reliability-based inspection, Struct. Saf. 22 (2) (2000) 145–160.
[26] S. Sankararaman, Y. Ling, S. Mahadevan, Statistical inference of equivalent initial flaw size with complicated structural geometry and multi-axial variable amplitude loading, Int. J. Fatig. 32 (10) (2010) 1689–1700.
[27] X. Guan, R. Jha, Y. Liu, Model selection, updating, and averaging for probabilistic fatigue damage prognosis, Struct. Saf. 33 (3) (2011) 242–249.
[28] S. Sankararaman, Y. Ling, S. Mahadevan, Uncertainty quantification and model validation of fatigue crack growth prediction, Eng. Fract. Mech. 78 (7) (2011) 1487–1504.
[29] A. Rodler, S. Guernouti, M. Musy, Bayesian inference method for in situ thermal conductivity and heat capacity identification: comparison to ISO standard, Construct. Build. Mater. 196 (2019) 574–593.
[30] M. Chiachío, J. Chiachío, G. Rus, J.L. Beck, Predicting fatigue damage in composites: a Bayesian framework, Struct. Saf. 51 (2014) 57–68.
[31] J. Chiachío, M. Chiachío, A. Saxena, S. Sankararaman, G. Rus, K. Goebel, Bayesian model selection and parameter estimation for fatigue damage progression models in composites, Int. J. Fatig. 70 (2015) 361–373.
[32] J.L. Beck, Bayesian system identification based on probability logic, Struct. Contr. Health Monit. 17 (7) (2010) 825–847.
[33] G. Rus, J. Chiachío, M. Chiachío, Logical inference for inverse problems, Inverse Probl. Sci. Eng. 24 (3) (2016) 448–464.
[34] K.V. Yuen, Recent developments of Bayesian model class selection and applications in civil engineering, Struct. Saf. 32 (5) (2010) 338–346.
[35] E.T. Jaynes, Information theory and statistical mechanics, Phys. Rev. 106 (4) (1957) 620.
[36] N. Metropolis, A.W. Rosenbluth, M.N. Rosenbluth, A.H. Teller, E. Teller, Equation of state calculations by fast computing machines, J. Chem. Phys. 21 (6) (1953) 1087–1092.
[37] W.K. Hastings, Monte Carlo sampling methods using Markov chains and their applications, Biometrika 57 (1) (1970) 97–109.
[38] L.L.C. Agisoft, Agisoft Metashape User Manual, Professional Edition, 2019. Version 1.5, St. Petersburg.
[39] D. Girardeau-Montaut, CloudCompare, EDF R&D Telecom ParisTech, 2016.
[40] A. Gelman, G.O. Roberts, W.R. Gilks, Efficient Metropolis jumping rules, Bayesian Stat. 5 (599–608) (1996) 42.
[41] G.O. Roberts, J.S. Rosenthal, Optimal scaling for various Metropolis-Hastings algorithms, Stat. Sci. 16 (4) (2001) 351–367.